

Supporting Information

Structural cutting and recombining in a layered sodium dysprosium phosphonate: key roles of flexible pyrazinyl hydrazone molecular tools[†]

Xiao Sun,^a Peiqiong Chen,^a Yanan Liu,^a Hou-Ting Liu^{*a} and Haiquan Tian^{*a}

^a Shandong Provincial Key Laboratory of Chemical Energy Storage and Novel Cell Technology, School of Chemistry and Chemical Engineering, Liaocheng University, Liaocheng 252059, P. R. China. E-mail: tianhaiquan@lcu.edu.cn, liuhouting@lcu.edu.cn

Table S1. Selected bond lengths (Å) and angles (°) for **1**.

Compound 1							
Dy1–O1	2.334(9)	Dy6···Na3	3.7346(1)	Dy5···Na3	3.7524(1)	Dy3···Na1	9.9315(3)
Dy1–O2	2.247(10)	Dy6···Na3	7.8328(3)	Dy5···Na1	7.3023(2)	Dy4···Na5	3.9729(1)
Dy1–O13	2.378(8)	Dy2–N5	3.1187(2)	Dy6···Na1	3.7841(1)	Dy4···Na3	9.4972(3)
Dy1–O19	2.493(8)	Dy3–O4	2.347(9)	Dy6···Na4	8.1641(3)	Dy5···Dy6	3.9638(1)
Dy1–O20	2.288(9)	Dy3–O5	2.274(10)	Dy4–N16	2.505(12)	Dy5···Na2	9.2912(3)
Dy1–O22	2.303(9)	Dy3–O7	2.340(8)	Dy5–O16	2.392(9)	Dy6···Na5	6.5693(2)
Dy1–N4	2.514(13)	Dy3–O26	2.271(9)	Dy5–O21	2.343(10)	Na1···Na3	7.3825(3)
Dy1–N17	2.532(11)	Dy3–O27	2.462(8)	Dy5–O23	2.460(9)	Na1···Na2	9.0417(3)
Dy2–O1	2.828(9)	Dy3–O28	2.342(10)	Dy5–O24	2.461(9)	Na2···Na4	7.0537(2)
Dy2–O4	2.758(9)	Dy3–N8	2.561(10)	Dy5–O30	2.196(9)	Na3···Na4	9.5088(3)
Dy2–O20	3.1070(1)	Dy3–N9	2.596(11)	Dy5–O33	2.366(10)	Na1···Na3	9.0770(3)
Dy2–O22	2.9914(1)	Dy4–O7	2.484(8)	Dy5–N21	2.598(13)	Na1···Na5	9.4702(3)
Dy2–O23	2.8837(2)	Dy4–O8	2.250(10)	Dy6–O13	2.487(8)	Na3···Na5	6.4419(2)
Dy2–O26	3.0751(3)	Dy4–O10	2.393(9)	Dy6–O14	2.276(8)	Na2···Na5	7.1192(2)
Dy2–O28	2.8712(1)	Dy4–O11	2.259(10)	Dy6–O16	2.416(7)	Na4···Na5	3.0644(1)
Dy2–N1	3.1168(2)	Dy4–O27	2.380(8)	Dy6–O17	2.239(10)	Dy1–O1–Dy2	103.2(3)
Na1–O2	2.415(11)	Dy4–O29	2.298(9)	Dy6–O19	2.323(8)	Dy1–O2–Na1	105.1(4)
Na1–O3	2.375(13)	Dy4–N12	2.570(11)	Dy6–O24	2.348(8)	Dy3–O7–Na2	99.9(3)
Na1–O13	2.506(11)	Na3–O36	2.378(19)	Dy6–N20	2.557(13)	Dy4–O10–Na4	89.2(4)
Na1–O17	2.319(11)	Na4–O8	2.397(12)	Dy6–N24	2.556(11)	Dy4–O11–Na2	108.7(4)
Na1–O18	2.519(12)	Na4–O10	2.490(13)	P2–O23	1.524(10)	Dy6–O13–Na1	98.6(3)
Na1–O34	2.292(12)	Na4–O29	2.453(11)	P2–O24	1.531(9)	Dy5–O16–Na3	100.5(4)
Na2–O5	2.380(11)	Na4–O31	2.600(15)	P2–C89	1.789(15)	Dy1–O19–Dy6	114.0(4)
Na2–O6	2.335(13)	Na4–O37	2.69(3)	P3–O25	1.459(10)	Dy3–O27–Dy4	111.6(3)
Na2–O7	2.535(10)	Na5–O10	2.291(12)	P3–O26	1.555(11)	Dy5–O31–Na5	97.0(5)
Na2–O11	2.299(11)	Na5–O23	2.302(12)	P3–O27	1.540(8)	Dy2–O4–Dy3	102.8(3)
Na2–O12	2.400(13)	Na5–O25	2.543(13)	P3–C99	1.878(19)	Dy4–O7–Na2	95.1(3)
Na2–O35	2.295(12)	Na5–O31	2.127(14)	P4–O28	1.521(11)	Dy4–O10–Na5	116.0(4)
Na3–O14	2.401(11)	Na5–N13	2.500(16)	P4–O29	1.516(9)	Dy1–O13–Dy6	112.3(3)
Na3–O15	2.235(12)	P1–O19	1.545(10)	P4–O30	1.526(10)	Dy6–O14–Na3	105.9(4)
Na3–O16	2.488(9)	P1–O20	1.522(11)	P4–C109	1.809(15)	Dy6–O16–Na3	99.2(3)
Na3–O33	2.238(14)	P1–O21	1.502(10)	P5–O31	1.540(13)	Dy5–O23–Na5	90.6(3)
Dy1···Dy6	4.0403(1)	P1–C79	1.785(15)	P5–O32	1.458(14)	Dy4–O29–Na4	92.3(4)
Dy1···Na5	6.8952(2)	P2–O22	1.514(9)	P5–O33	1.548(12)	Na4–O31–Na5	80.2(5)
Dy1···Na4	9.3144(3)	Dy1···Dy2	4.0562(1)	P5–C119	1.856(18)	Dy3–O5–Na2	106.7(4)
Dy2···Dy5	4.2016(1)	Dy1···Na3	7.3664(3)	Dy1···Na1	3.7016(1)	Dy4–O8–Na4	95.0(4)
Dy2···Dy4	6.1982(2)	Dy1···Na2	9.9431(3)	Dy1···Dy5	5.4053(2)	Na4–O10–Na5	79.6(4)
Dy2···Na2	7.5940(2)	Dy2···Na5	4.2297(1)	Dy1···Dy3	8.0166(2)	Dy1–O13–Na1	98.6(3)
Dy3···Dy4	4.0040(1)	Dy2···Na4	6.5205(2)	Dy2···Dy3	3.9970(1)	Dy5–O16–Dy6	111.1(3)
Dy3···Dy5	6.6637(2)	Dy2···Na3	7.7451(2)	Dy2···Dy6	6.0670(2)	Dy6–O17–Na1	112.2(5)
Dy4···Na4	3.4268(1)	Dy3···Na5	5.1605(2)	Dy2···Na1	7.5794(2)	Dy5–O24–Dy6	111.0(3)
Dy4···Dy5	6.3877(2)	Dy3···Dy6	9.7190(3)	Dy3···Na2	3.7341(1)	Dy5–O31–Na4	124.3(5)
Dy5···Na5	3.3855(1)	Dy4···Na2	3.7043(1)	Dy3···Na4	6.3243(2)	Dy5–O33–Na3	109.1(5)
Dy5···Na4	4.4111(1)	Dy4···Na4	9.4243(3)				

Table S2. Selected bond lengths (Å) and angles (°) for **2**.

Compound 2							
Dy1–O20	2.293(13)	Dy4–O46	2.405(15)	P3–O39	1.522(16)	Na1–O43	2.60(2)
Dy1–O22	2.327(13)	Dy4–O47	2.383(13)	P3–O40	1.49(2)	Na1–O49	2.39(3)
Dy1–O27	2.314(17)	Dy5–O17	2.33(2)	P3–C22	1.87(2)	Na2–O7	2.37(2)
Dy1–O28	2.290(16)	Dy5–O18	2.280(14)	P4–O22	1.522(15)	Na2–O8	2.513(17)
Dy1–O44	2.421(16)	Dy5–O28	2.465(15)	P4–O23	1.484(17)	Na2–O29	2.493(18)
Dy1–O46	2.332(14)	Dy5–O29	2.408(14)	P4–O24	1.528(14)	Na2–O31	2.711(18)
Dy1–O47	2.334(14)	Dy5–O31	2.237(14)	P4–C32	1.810(16)	Na2–O33	2.520(19)
Dy2–O9	2.456(15)	Dy5–O36	2.259(14)	P5–O35	1.533(15)	Na2–O34	2.38(3)
Dy2–O10	2.267(17)	Dy5–O47	2.431(14)	P5–O36	1.510(17)	Na2–N6b	2.72(2)
Dy2–O12	2.382(17)	Dy6–O3	2.470(17)	P5–O37	1.479(17)	Na3–O4	2.41(2)
Dy2–O24	2.290(14)	Dy6–O5	2.264(17)	Na3–N2d	2.67(2)	Na4–O15	2.64(2)
Dy2–O39	2.230(14)	Dy6–O6	2.40(2)	Na4–O10	2.430(17)	Na4–O23	2.692(17)
Dy2–O48	2.472(12)	Dy6–O19	2.280(15)	Na4–O11	2.36(2)	Na4–O24	2.594(19)
Dy2–N1	2.601(16)	Dy6–O21	2.473(15)	Na4–O40	2.49(2)	Dy7–O15–Na4	86.6(7)
Dy2–N8	2.501(17)	Dy6–O37	2.247(14)	Dy1⋯Dy2	5.7425(13)	Dy6–O6–Dy8	104.2(7)
Dy3–O8	2.230(17)	Dy6–N11	2.645(19)	Dy1⋯Dy3	5.7731(13)	Dy6–O19–Na3	96.2(6)
Dy3–O9	2.370(16)	Dy6–N15	2.49(2)	Dy1⋯Dy4	3.8799(13)	Dy6–O21–Dy8	98.7(4)
Dy3–O12	2.433(15)	Dy7–O14	2.66(2)	Dy1⋯Dy5	3.8094(13)	Dy5–O36–Na3	96.6(6)
Dy3–O30	2.258(13)	Dy7–O15	2.43(2)	Dy1⋯Dy6	5.8121(14)	Dy7–O40–Na4	94.0(6)
Dy3–O33	2.310(15)	Dy7–O23	2.327(14)	Dy1⋯Dy7	3.8596(14)	Dy2–O9–Dy3	103.2(5)
Dy3–O48	2.472(12)	Dy7–O26	2.426(16)	Dy1⋯Dy8	5.8359(14)	Dy2–O10–Na4	99.1(6)
Dy3–N4	2.472(17)	Dy7–O27	2.480(15)	Dy2⋯Dy3	3.7839(13)	Dy2–O12–Dy3	103.6(5)
Dy3–N5	2.609(17)	Dy7–O40	2.271(16)	Dy2⋯Dy4	5.6291(13)	Dy7–O14–Na1	88.2(8)
Dy4–O32	2.274(14)	Dy7–O43	2.254(16)	Dy2⋯Dy5	7.3551(18)	Dy6–O5–Na3	98.6(6)
Dy4–O35	2.312(16)	Dy7–O46	2.494(17)	Dy2⋯Dy6	9.3316(16)	Dy5–O18–Na3	94.9(6)
Dy4–O38	2.273(16)	Dy8–O2	2.22(2)	Dy2⋯Dy7	5.4327(13)	Dy3–O33–Na2	96.0(6)
Dy4–O41	2.257(16)	Dy8–O3	2.344(16)	Dy3⋯Dy4	6.0339(13)	Dy7–O23–Na4	87.7(5)
Dy4–O45	2.347(16)	Dy8–O6	2.39(2)	Dy3⋯Dy5	5.4486(14)	Dy2–O24–Na4	94.0(5)
Dy8–O21	2.505(16)	P6–C52	1.839(16)	Dy3⋯Dy7	7.6393(18)	Dy7–O26–Na1	96.4(7)
Dy8–O25	2.268(17)	P7–O41	1.54(2)	Dy4⋯Dy5	4.2939(13)	Dy1–O27–Dy7	107.2(5)
Dy8–O42	2.217(17)	P7–O42	1.506(17)	Dy4⋯Dy6	5.6412(14)	Dy1–O28–Dy5	106.4(5)
Dy8–N9	2.43(2)	P7–O43	1.48(2)	Dy4⋯Dy7	4.3789(13)	Dy5–O29–Na2	103.6(6)
Dy8–N12	2.62(3)	P7–C62	1.767(18)	Dy4⋯Dy8	5.9576(14)	Dy1–O46–Dy7	106.2(5)
P1–O31	1.498(15)	P8–O25	1.490(15)	Dy5⋯Dy6	5.4598(14)	Dy5–O31–Na2	101.8(6)
P1–O32	1.540(19)	P8–O26	1.553(19)	Dy5⋯Dy7	7.1309(18)	Dy1–O47–Dy5	106.1(5)
P1–O33	1.495(14)	P8–O27	1.543(16)	Dy5⋯Dy8	7.6029(18)	Dy8–O42–Na1	95.2(7)
P1–C1	1.803(19)	P8–C72	1.843(18)	Dy6⋯Dy7	7.3901(18)	Dy7–O43–Na1	96.7(7)
P2–O28	1.568(16)	Na1–O1	2.44(3)	Dy6⋯Dy8	3.7774(18)	Dy1–O46–Dy4	110.0(6)
P2–O29	1.521(18)	Na1–O2	2.48(2)	Dy7⋯Dy8	5.3935(16)	Dy4–O46–Dy7	126.7(6)
P2–O30	1.500(14)	Na1–O14	2.56(2)	Dy3–O8–C93	137.9(16)	Dy1–O47–Dy4	110.7(6)
P2–C11	1.817(17)	Na1–O26	2.44(2)	Dy8–O2–Na1	100.8(8)	Dy4–O47–Dy5	126.3(6)
P3–O38	1.515(16)	Na1–O42	2.68(2)	Dy6–O3–Dy8	103.4(6)	Dy2–O48–Dy3	99.9(3)

Table S3. Hydrogen bonds in **1**.

Compound 1				
D–H···A	d(D–H) (Å)	d(H···A) (Å)	d(D···A) (Å)	<(DHA) (°)
O34–H34b···N10	0.8500	2.1500	2.81(2)	134.00
O34–H34c···N2	0.8500	2.5200	2.944(16)	112.00
O35–H35b···N18	0.8500	2.5600	2.851(19)	101.00
O35–H35c···N6	0.8500	2.1700	2.912(17)	145.00
O37–H37b···O32	0.8500	2.3000	2.77(3)	115.00
C1–H1···O26	0.9300	2.3800	3.081(19)	132.00
C129–H12a···O36	0.9600	1.9600	2.78(5)	142.00
C129–H12c···O32	0.9600	2.0200	2.71(5)	126.00
C14–H14···O20	0.9300	2.3100	3.01(2)	132.00
C42–H42···N15	0.9300	2.4400	2.77(2)	101.00
C55–H55···N19	0.9300	2.4900	2.80(2)	100.00
C80–H80···O21	0.9300	2.4900	2.899(19)	107.00
C82–H82···N15	0.9300	2.6100	3.36(3)	139.00
C87–H87···O19	0.9300	2.4400	3.016(19)	120.00
C90–H90···O24	0.9300	2.5200	2.95(2)	108.00
C97–H97···O22	0.9300	2.2700	2.96(2)	131.00
C100–H100···O27	0.9300	2.3800	2.87(2)	112.00
C110–H110···O29	0.9300	2.5500	2.96(2)	107.00
C117–H117···O28	0.9300	2.3700	3.07(2)	132.00
C120–H120···O33	0.9300	2.5200	2.94(2)	108.00
C127–H127···O32	0.9300	2.3700	3.04(3)	130.00

Symmetry codes: (a) x, y, -1+z; (b) -x, -y, -z; (c) 1+x, y, z.

Table S4. Hydrogen bonds in **2**.

Compound 2				
D–H···A	d(D–H) (Å)	d(H···A) (Å)	d(D···A) (Å)	<(DHA) (°)
O13–H13b···N16	0.8500	2.2600	2.82(3)	124.00
O34–H34a···O17	0.8500	2.2200	2.78(3)	124.00
C2–H2···O31	0.9300	2.4200	2.86(2)	109.00
C12–H12···O30	0.9300	2.4600	2.89(2)	108.00
C120–H12a···O16	0.9600	2.4000	3.21(4)	141.00
C17–H17···O29	0.9300	2.2500	3.00(3)	137.00
C23–H23···O39	0.9300	2.5400	2.92(3)	104.00
C28–H28···O40	0.9300	2.2800	3.05(3)	140.00
C33–H33···O23	0.9300	2.3600	2.84(2)	112.00
C40–H40···O9	0.9300	2.6000	3.36(2)	139.00
C43–H43···O36	0.9300	2.4500	2.86(3)	107.00
C50–H50···O37	0.9300	2.3900	3.13(3)	136.00
C53–H53···O18	0.9300	2.4800	2.92(2)	109.00
C60–H60···O20	0.9300	2.5500	3.18(2)	125.00
C63–H63···O43	0.9300	2.4000	2.85(3)	110.00
C73–H73···O27	0.9300	2.5100	2.96(2)	110.00
C8–H80···O25	0.9300	2.4000	3.01(3)	123.00
C82–H82···O10	0.9300	2.4900	3.07(2)	121.00
C94–H94a···O34	0.9600	2.3900	3.15(4)	135.00
C96–H96···O33	0.9300	2.5400	3.27(3)	136.00
C121–H121···O5	0.9300	2.5800	3.14(3)	119.00

Symmetry codes: (a) -x, 2-y, -z; (b) x, -1+y, z.

Table S5. Dy^{III} and Na^I geometry analysis of **1** by SHAPE 2.1 software.

Dy									
Geometry (CN = 8)		Dy1	Dy3	Dy4	Dy5	Dy6	Geometry (CN = 10)		Dy2
TDD-8		3.061	2.881	3.125	2.712	2.573	PARP-10		3.431
BTPR-8		3.110	3.090	2.123	2.679	2.472	SDD-10		5.613
JSD-8		3.485	3.538	3.282	5.988	2.319	HD-10		6.591
JBTPR-8		4.248	4.312	2.670	3.571	3.149	TD-10		7.416
SAPR-8		5.341	4.772	3.942	4.377	5.007	JMBIC-10		7.547
JGBF-8		9.787	9.786	10.082	12.443	9.223	JBCCU-10		9.655
CU-8		11.616	12.003	9.334	10.367	12.614	PPR-10		9.834
TT-8		12.189	12.582	9.774	10.998	13.262	JSPC-10		12.936
HBPY-8		12.885	12.723	12.507	13.921	14.016	JBCSAPR-10		13.388
ETBPY-8		21.041	21.636	20.191	21.739	20.115	JATDI-10		14.600
JETBPY-8		25.982	26.470	24.577	24.200	24.309	OBPY-10		15.740
HPY-8		24.390	25.016	24.114	21.173	24.088	EPY-10		24.156
OP-8		31.937	30.971	31.950	34.252	32.016	DP-10		25.993
Na									
Geometry (CN = 6)		Na1	Na2	Na5	Geometry (CN = 5)		Na3	Geometry (CN = 7)	
HP-6		26.359	27.495	34.288	PP-5		18.038	HP-7	
PPY-6		12.386	12.507	16.956	vOC-5		5.122	HPY-7	
OC-6		8.447	8.638	7.886	TBPY-5		8.825	PBPY-7	
TPR-6		8.871	7.109	8.880	SPY-5		5.402	COC-7	
JPPY-6		15.606	15.995	20.965	JTBPY-5		11.374	CTPR-7	
								JPBPY-7	
								JETPY-7	
Lable	Shape	Lable	Shape	Lable	Shape	Lable	Shape	Lable	Shape
PP-5	Pentagon (D _{5h})	JPPY-6	Johnson pentagonal pyramid (C _{5v})	HPY-8	Heptagonal pyramid (C _{7v})	JSD-8	Snub diphenoid J84 (D _{2d})	JMBIC-10	Metabidiminished icosahedron (J62) (C _{2v})
vOC-5	Vacant octahedron‡ (Johnson square pyramid, J1) (C _{4v})	HP-7	Heptagon	HBPY-8	Hexagonal bipyramid (D _{6h})	TT-8	Triakis tetrahedron (T _d)	JATDI-10	Augmented tridiminished icosahedron (J64) (C _{3v})
TBPY-5	Trigonal bipyramid (D _{3h})	HPY-7	Hexagonal pyramid (C _{6v})	CU-8	Cube (O _h)	DP-10	Decagon (D _{10h})	JSPC-10	Sphenocorona (J87) (C _{2v})
SPY-5	Square pyramid [§] (C _{4v})	PBPY-7	Pentagonal bipyramid (D _{5h})	SAPR-8	Square antiprism (D _{4d})	EPY-10	Enneagonal pyramid (C _{9v})	SDD-10	Staggered dodecahedron (2:6:2) # (D ₂)
JTBPY-5	Johnson trigonal bipyramid (J12) (D _{3h})	COC-7	Capped octahedron (C _{3v})	TDD-8	Triangular dodecahedron (D _{2d})	OBPY-10	Octagonal bipyramid (D _{8h})	TD-10	Tetradecahedron (2:6:2) (C _{3v})
HP-6	Hexagon (D _{6h})	CTPR-7	Capped trigonal prism (C _{2v})	JGBF-8	Johnson gyrobiafastigium J26 (D _{2d})	PPR-10	Pentagonal prism (D _{5h})	HD-10	Hexadecahedron (2:6:2, or 1:4:4:1) (D _{4h})
PPY-6	Pentagonal pyramid (C _{5v})	JPBPY-7	Johnson pentagonal bipyramid J13 (D _{5h})	JETBPY-8	Johnson elongated triangular bipyramid J14 (D _{3h})	PAPR-10	Pentagonal antiprism (D _{5d})		
OC-6	Octahedron (O _h)	JETPY-7	Elongated triangular pyramid J7 (C _{3v})	JBTPR-8	Biaugmented trigonal prism J50 (C _{2v})	JBCCU-10	Bicapped cube (Elongated square bipyramid J15) (D _{4h})		
TPR-6	Trigonal prism (D _{3h})	OP-8	Octagon (D _{8h})	BTPR-8	Biaugmented trigonal prism (C _{2v})	JBCSAPR-10	Bicapped square antiprism (Gyroelongated square bipyramid J17) (D _{4d})		

Table S6. Dy^{III} and Na^I geometry analysis of **2** by SHAPE 2.1 software.

Dy									
Geometry (CN = 7)	Dy1	Dy4	Dy5	Geometry (CN = 8)	Dy2	Dy3	Dy6	Dy7	Dy8
HP-7	35.140	33.262	30.045	OP-8	32.863	34.037	32.526	29.539	32.257
HPY-7	19.787	23.957	22.079	HPY-8	23.889	23.451	23.807	20.769	23.056
PBPY-7	4.526	0.358	2.156	HBPY-8	15.735	15.840	15.359	10.740	15.858
COC-7	2.285	7.096	3.866	CU-8	12.397	12.223	12.212	12.137	11.049
CTPR-7	1.462	5.262	2.228	SAPR-8	3.183	3.668	3.146	6.316	3.462
JPBPY-7	8.185	3.336	4.986	TDD-8	2.379	2.515	2.184	5.059	1.990
JETPY-7	20.286	22.968	20.255	JGBF-8	14.038	13.728	13.488	7.332	13.413
				JETBPY-8	28.107	28.080	28.195	20.574	27.329
				JBTPR-8	2.721	3.138	2.720	3.891	2.892
				BTPR-8	2.195	2.541	2.135	3.892	2.424
				JSD-8	4.441	4.662	4.161	4.432	4.067
				TT-8	13.141	13.012	12.903	12.695	11.606
				ETBPY-8	24.918	24.641	24.854	17.863	23.820
Na									
Geometry (CN = 7)	Na1		Na2		Na3		Na4		
HP-7	30.889		31.509		32.008		29.778		
HPY-7	15.241		21.702		21.498		15.571		
PBPY-7	6.061		2.851		2.381		4.913		
COC-7	5.580		5.065		5.748		5.567		
CTPR-7	4.625		3.240		4.420		4.760		
JPBPY-7	8.505		7.280		7.153		7.080		
JETPY-7	16.747		19.396		20.232		16.235		
Lable	Shape	Lable	Shape	Lable	Shape	Lable	Shape	Lable	Shape
HP-7	Heptagon	CTPR-7	Capped trigonal prism (C _{2v})	OP-8	Octagon (D _{8h})	SAPR-8	Square antiprism (D _{4d})	JBTPR-8	Biaugmented trigonal prism J50 (C _{2v})
HPY-7	Hexagonal pyramid (C _{6v})	JPBPY-7	Johnson pentagonal bipyramid J13 (D _{5h})	HPY-8	Heptagonal pyramid (C _{7v})	TDD-8	Triangular dodecahedron (D _{2d})	BTPR-8	Biaugmented trigonal prism (C _{2v})
PBPY-7	Pentagonal bipyramid (D _{5h})	JETPY-7	Elongated triangular pyramid J7 (C _{3v})	HBPY-8	Hexagonal bipyramid (D _{6h})	JGBF-8	Johnson gyrobifastigium J26 (D _{2d})	JSD-8	Snub diphenoid J84 (D _{2d})
COC-7	Capped octahedron (C _{3v})			CU-8	Cube (O _h)	JETBPY-8	Johnson elongated triangular bipyramid J14 (D _{3h})	TT-8	Triakis tetrahedron (T _d)

Table S7. Relaxation fitting parameters from least-squares fitting of $\chi(\omega)$ data under zero dc field for **1** (1.0-1000 Hz).

		$\text{Ln}(\chi''/\chi')$							
T (k) V (Hz)	1.8	2.0	2.3	2.6	2.9	3.2	3.5	3.8	4.1
1.000(5)	-5.049(9)	-5.183(5)	-5.263(1)	-5.337(5)	-5.392(8)	-5.429(8)	-5.483(2)	-5.521(4)	-5.546(1)
17.193(1)	-4.972(1)	-5.095(3)	-5.196(1)	-5.256(7)	-5.324(5)	-5.382(7)	-5.396(8)	-5.457(1)	-5.512(3)
21.046(6)	-4.851(4)	-4.989(2)	-5.090(6)	-5.162(8)	-5.203(7)	-5.279(4)	-5.314(1)	-5.356(4)	-5.371(2)
25.807(6)	-4.730(7)	-4.854(3)	-4.936(5)	-5.014(4)	-5.075(2)	-5.123(9)	-5.166(7)	-5.196(3)	-5.239(1)
31.624(4)	-4.608(9)	-4.728(7)	-4.809(6)	-4.876(2)	-4.939(8)	-4.979(1)	-5.010(6)	-5.067(2)	-5.096(8)
38.752(4)	-4.507(2)	-4.621(7)	-4.702(2)	-4.782(4)	-4.834(2)	-4.880(2)	-4.931(8)	-4.962(2)	-5.001(1)
47.498(1)	-4.436(7)	-4.549(9)	-4.643(6)	-4.717(8)	-4.766(5)	-4.811(1)	-4.869(6)	-4.899(5)	-4.927(1)
58.128(7)	-4.369(8)	-4.492(1)	-4.581(4)	-4.648(8)	-4.722(1)	-4.768(1)	-4.807(1)	-4.855(6)	-4.898(9)
71.178(1)	-4.302(2)	-4.423(6)	-4.513(1)	-4.589(7)	-4.649(4)	-4.703(1)	-4.754(1)	-4.792(1)	-4.839(1)
87.349(1)	-4.202(2)	-4.326(9)	-4.424(5)	-4.501(9)	-4.566(9)	-4.617(2)	-4.658(9)	-4.703(6)	-4.743(1)
107.079(2)	-4.095(6)	-4.216(8)	-4.314(4)	-4.390(6)	-4.452(5)	-4.509(4)	-4.549(1)	-4.591(1)	-4.626(8)
130.906(4)	-3.978(2)	-4.103(3)	-4.192(2)	-4.263(9)	-4.330(1)	-4.381(1)	-4.428(1)	-4.464(9)	-4.505(9)
160.618(8)	-3.860(7)	-3.982(1)	-4.070(7)	-4.138(5)	-4.201(8)	-4.257(1)	-4.292(9)	-4.333(2)	-4.366(2)
196.887(6)	-3.748(5)	-3.872(1)	-3.961(6)	-4.026(7)	-4.088(7)	-4.136(9)	-4.178(1)	-4.214(1)	-4.249(1)
241.126(5)	-3.647(1)	-3.772(4)	-3.856(4)	-3.923(8)	-3.985(4)	-4.037(3)	-4.074(5)	-4.110(4)	-4.141(7)
295.480(3)	-3.553(4)	-3.675(3)	-3.766(6)	-3.845(6)	-3.897(8)	-3.950(1)	-3.983(1)	-4.020(9)	-4.056(1)
362.360(8)	-3.462(8)	-3.586(2)	-3.683(6)	-3.753(9)	-3.809(9)	-3.864(8)	-3.906(7)	-3.938(2)	-3.972(6)
443.892(1)	-3.375(4)	-3.504(1)	-3.595(4)	-3.679(1)	-3.731(5)	-3.785(9)	-3.826(8)	-3.861(6)	-3.896(6)
544.045(9)	-3.287(3)	-3.422(8)	-3.518(3)	-3.594(6)	-3.658(5)	-3.708(4)	-3.750(7)	-3.784(9)	-3.817(2)
666.595(5)	-3.203(8)	-3.338(6)	-3.435(2)	-3.514(5)	-3.574(2)	-3.620(6)	-3.662(6)	-3.697(1)	-3.734(1)
815.501(1)	-3.129(4)	-3.266(1)	-3.366(5)	-3.449(9)	-3.513(2)	-3.567(5)	-3.607(2)	-3.635(9)	-3.682(1)
999.040(9)	-3.076(2)	-3.219(6)	-3.322(1)	-3.407(1)	-3.469(2)	-3.522(1)	-3.564(6)	-3.601(6)	-3.632(4)

Table S8. Relaxation fitting parameters from least-squares fitting of $\chi(\omega)$ data under zero *dc* field for **1** (10-10000 Hz).

<i>T</i>	χ_r	χ_s	α	τ / s
1.9	63.710(2)	36.288(3)	0.320(9)	1.995(9)E-5
2.5	60.250(7)	39.749(2)	0.299(7)	1.862(1)E-5
3.0	58.435(3)	41.564(6)	0.291(9)	1.707(1)E-5
3.5	56.968(1)	43.031(9)	0.282(9)	1.621(3)E-5
4.0	55.808(6)	44.191(3)	0.271(9)	1.586(6)E-5
4.5	55.190(7)	44.809(2)	0.287(6)	1.484(7)E-5
5.0	54.155(5)	45.844(4)	0.255(3)	1.416(2)E-5
7.0	51.908(5)	47.091(4)	0.242(7)	1.216(9)E-5
8.0	50.385(1)	48.614(8)	0.221(1)	1.081(2)E-5
9.0	48.834(5)	50.165(4)	0.206(8)	9.622(2)E-6
10.0	46.148(8)	52.148(8)	0.191(3)	9.046(1)E-6
11.0	44.690(7)	53.690(7)	0.179(1)	8.377(6)E-6
12.0	42.359(1)	54.640(9)	0.169(1)	7.375(1)E-6
13.0	40.385(4)	56.034(7)	0.151(6)	6.238(5)E-6
14.0	38.680(8)	58.059(2)	0.144(9)	5.411(7)E-6
15.0	36.561(5)	60.084(7)	0.128(4)	4.058(1)E-6
16.0	34.768(2)	61.809(2)	0.118(6)	3.112(8)E-6
17.0	32.757(3)	63.127(9)	0.106(9)	2.861(2)E-6
18.0	31.647(3)	64.182(4)	0.083(3)	2.346(1)E-6
19.0	30.013(6)	65.187(1)	0.073(6)	2.088(1)E-6
20.0	28.761(1)	66.152(8)	0.059(6)	1.954(4)E-6

Table S9. Relaxation fitting parameters from least-squares fitting of $\chi(\omega)$ data under zero dc field for **2** (1.0-1000 Hz).

T	χ_r	χ_s	α	τ / s
1.8	38.146(3)	23.853(6)	0.229(1)	1.185(1)E-4
2.0	36.780(1)	25.219(9)	0.219(1)	1.051(1)E-4
2.3	35.837(2)	26.162(8)	0.212(4)	8.950(7)E-5
2.6	35.139(7)	26.860(2)	0.207(1)	8.064(9)E-5
2.9	34.564(2)	27.435(7)	0.200(2)	7.532(4)E-5
3.2	34.238(8)	27.761(1)	0.202(9)	6.614(1)E-5
3.5	33.865(2)	28.134(7)	0.199(3)	6.272(9)E-5
4	33.533(6)	28.466(3)	0.194(3)	6.058(3)E-5
4.3	33.319(9)	28.680(1)	0.194(2)	5.617(5)E-5
4.6	32.927(5)	29.072(4)	0.189(8)	5.269(7)E-5
4.9	32.787(1)	29.212(9)	0.197(2)	4.491(1)E-5
5.5	32.600(3)	29.399(7)	0.199(5)	3.885(4)E-5
6.0	32.424(7)	29.575(2)	0.199(1)	3.422(4)E-5
6.5	32.239(1)	29.760(8)	0.196(5)	2.876(4)E-5
7.0	32.516(1)	29.483(9)	0.213(8)	2.222(1)E-5
7.5	32.206(6)	29.793(3)	0.198(3)	1.735(6)E-5
8.0	32.308(8)	29.691(1)	0.204(5)	1.397(2)E-5
8.5	32.316(6)	29.683(3)	0.203(3)	1.164(6)E-5
9.0	32.234(5)	29.765(4)	0.189(3)	9.352(8)E-6
10.0	31.719(7)	29.480(2)	0.126(5)	7.063(4)E-6
11.0	31.558(7)	29.241(2)	0.167(9)	6.014(5)E-6
12.0	31.492(5)	30.507(4)	0.099(9)	5.079(5)E-6
13.0	31.421(5)	30.578(4)	0.083(8)	4.659(6)E-6
14.0	35.771(4)	26.228(5)	0.115(3)	4.026(2)E-6
15.0	35.687(8)	26.312(1)	0.102(3)	3.530(7)E-6
16.0	35.783(5)	26.216(4)	0.071(9)	3.005(9)E-6
17.0	35.672(7)	26.327(2)	0.067(7)	2.665(2)E-6
18.0	35.457(1)	26.542(9)	0.076(6)	2.310(7)E-6
19.0	35.322(8)	26.677(2)	0.080(4)	2.036(1)E-6
20.0	35.733(3)	26.266(6)	0.038(5)	1.813(3)E-6

Table S10. Relaxation fitting parameters from least-squares fitting of $\chi(\omega)$ data under zero dc field for **2** (10-10000 Hz).

T	χ_r	χ_s	α	τ / s
1.9	69.004(4)	30.995(5)	0.312(1)	5.847(2)E-5
2.5	63.456(8)	36.543(1)	0.293(1)	3.911(3)E-5
3.0	60.665(1)	39.334(8)	0.283(7)	3.129(7)E-5
3.5	58.692(2)	41.307(7)	0.277(7)	2.649(7)E-5
4.0	57.146(2)	42.853(7)	0.265(1)	2.325(4)E-5
4.5	56.006(3)	43.993(7)	0.259(1)	2.049(3)E-5
5.0	55.230(3)	44.769(6)	0.266(1)	1.736(5)E-5
7.0	54.071(3)	45.928(6)	0.278(1)	1.218(6)E-5
8.0	53.060(1)	46.939(8)	0.268(4)	9.450(6)E-6
9.0	52.130(6)	47.869(3)	0.240(6)	8.342(4)E-6
10.0	51.584(2)	48.415(7)	0.234(2)	7.528(6)E-6
11.0	51.037(1)	48.962(9)	0.193(2)	6.331(5)E-6
12.0	51.693(8)	48.306(1)	0.312(6)	5.252(4)E-6
13.0	50.957(3)	49.042(6)	0.263(9)	3.874(5)E-6
14.0	51.494(7)	48.505(2)	0.289(5)	2.879(3)E-7
15.0	50.421(4)	49.578(5)	0.192(1)	2.429(4)E-6
16.0	50.275(2)	49.724(7)	0.192(9)	1.831(6)E-6
17.0	50.347(9)	49.652(1)	0.408(6)	1.360(2)E-6
18.0	50.309(7)	49.690(2)	0.669(5)	1.005(1)E-6
19.0	50.099(9)	49.900(1)	0.210(3)	8.169(1)E-7
20.0	50.052(5)	49.947(4)	0.193(3)	6.166(5)E-7

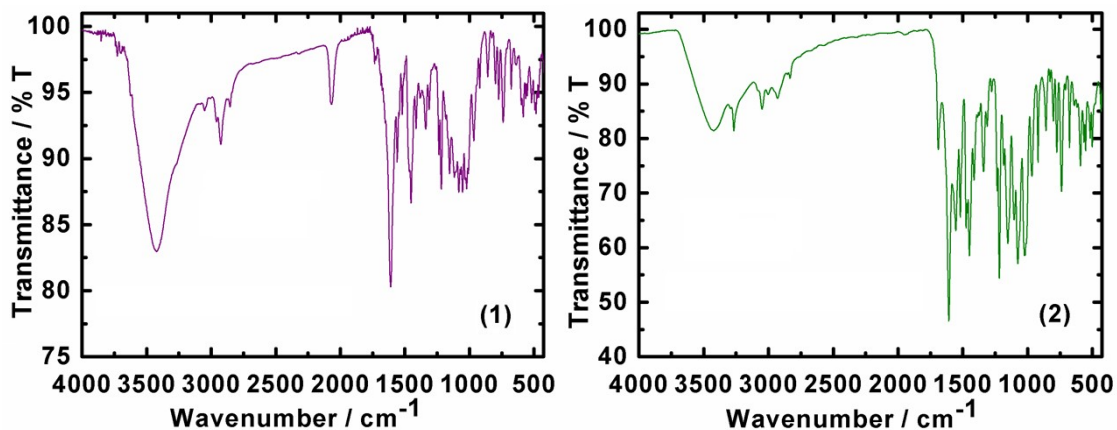


Figure S1. Infrared spectra of 1 (left) and 2 (right).

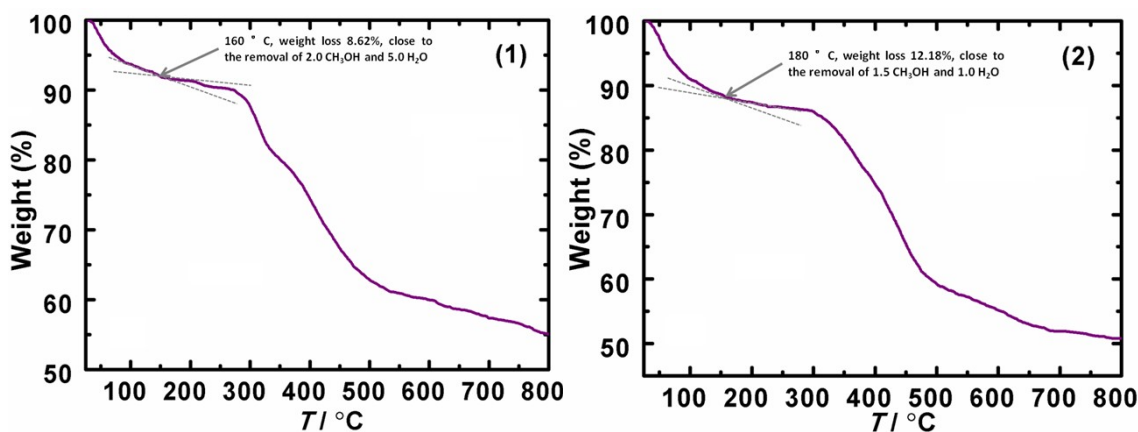


Figure S2. TG analyses of 1 (left) and 2 (right).

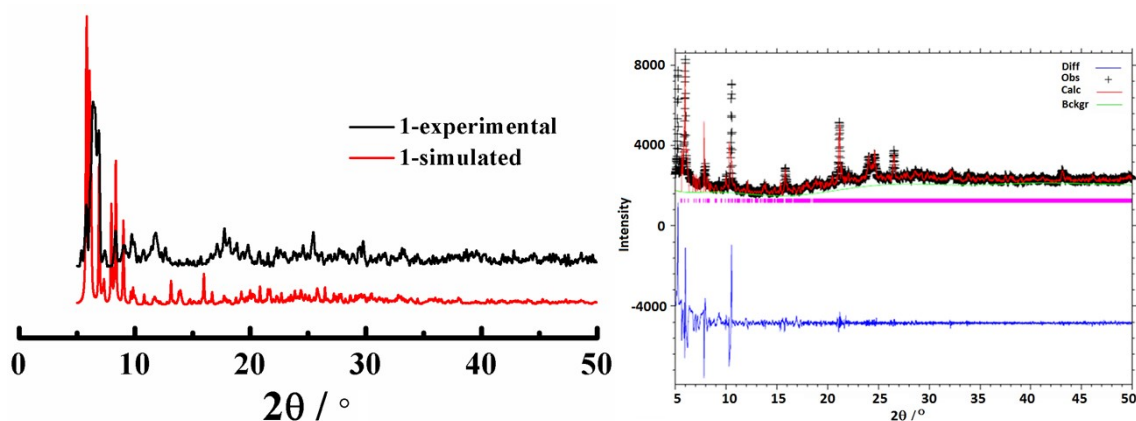


Figure S3. Left: the powder XRD patterns for compound 1. Right: the black circles are for the observed data. The red solid line is for the calculated data. The grey solid curve is for the difference. The vertical bars are the positions of Bragg peaks. Cell parameters: $P-1$, $a = 15.19 \text{ \AA}$, $b = 19.96 \text{ \AA}$, $c = 26.24 \text{ \AA}$, $\alpha = 89.5^\circ$, $\beta = 79.02^\circ$, $\gamma = 84.28^\circ$, $V = 7356.6 \text{ \AA}^3$ ($wRp = 0.114$).

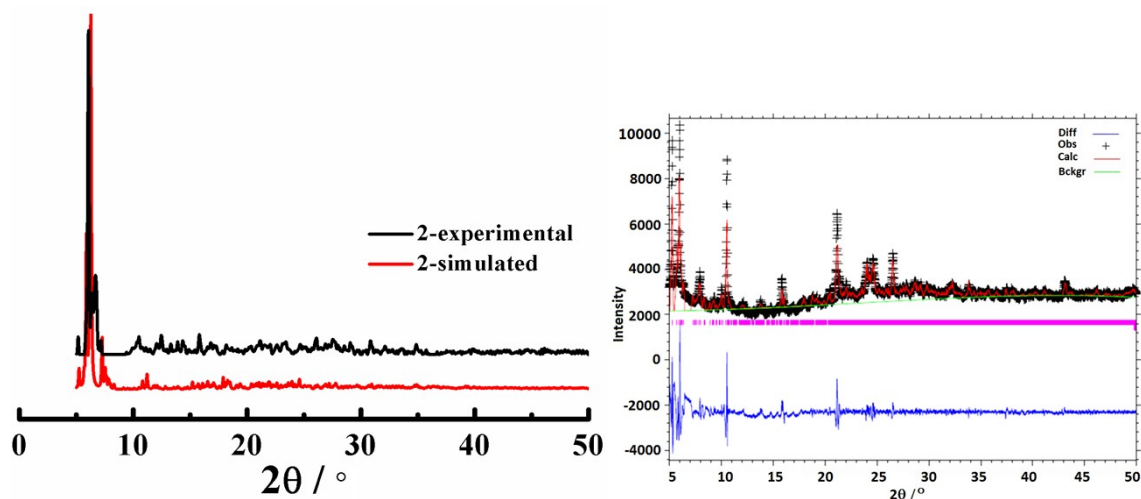
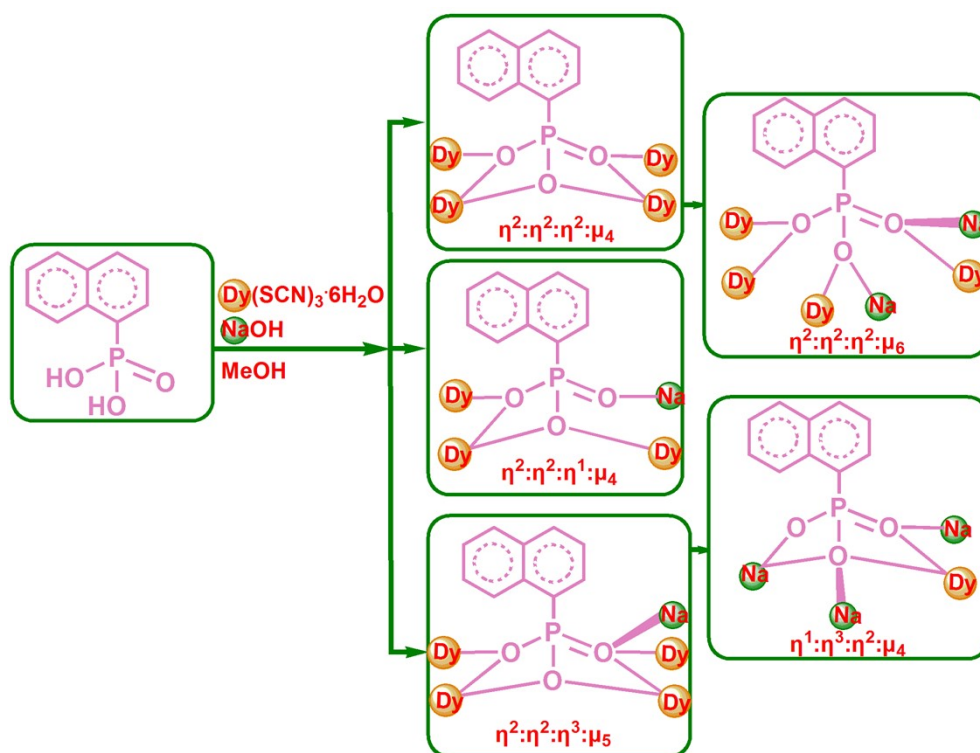
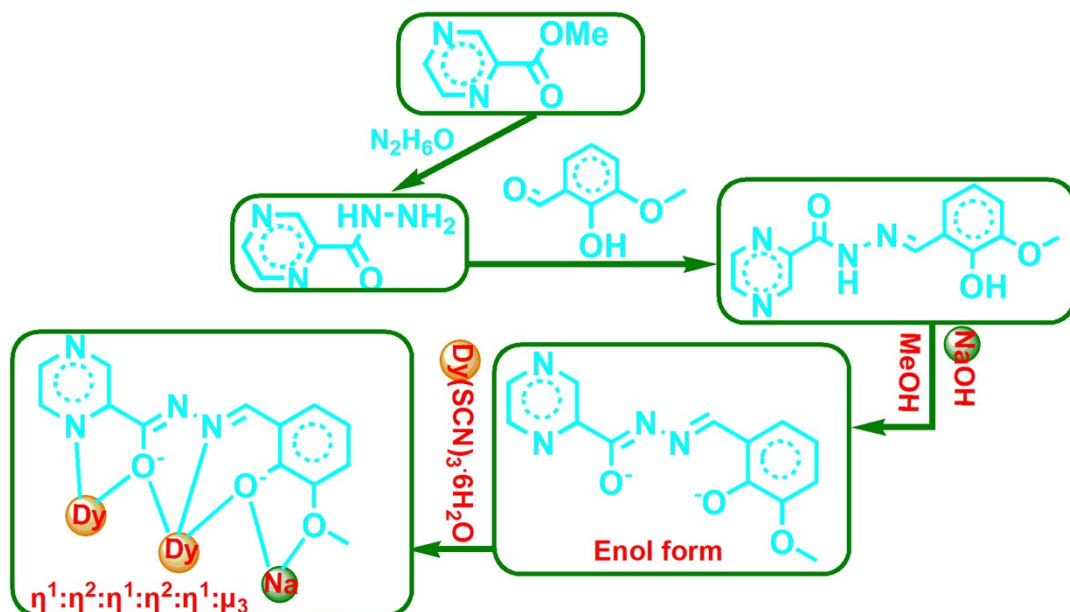


Figure S4. Left: the powder XRD patterns for compound **2**. Right: the black circles are for the observed data. The red solid line is for the calculated data. The grey solid curve is for the difference. The vertical bars are the positions of Bragg peaks. Cell parameters: $P2_1/c$, $a = 32.55 \text{ \AA}$, $b = 16.45 \text{ \AA}$, $c = 33.81 \text{ \AA}$, $\beta = 113.8^\circ$, $V = 16355.1 \text{ \AA}^3$ ($wRp = 0.069$).



Scheme S1. H_2opch , di-deprotonated opch^{2-} and corresponding coordination mode in **1**.



Scheme S2. H_2opch , di-deprotonated opch^{2-} and corresponding coordination mode in **1**.

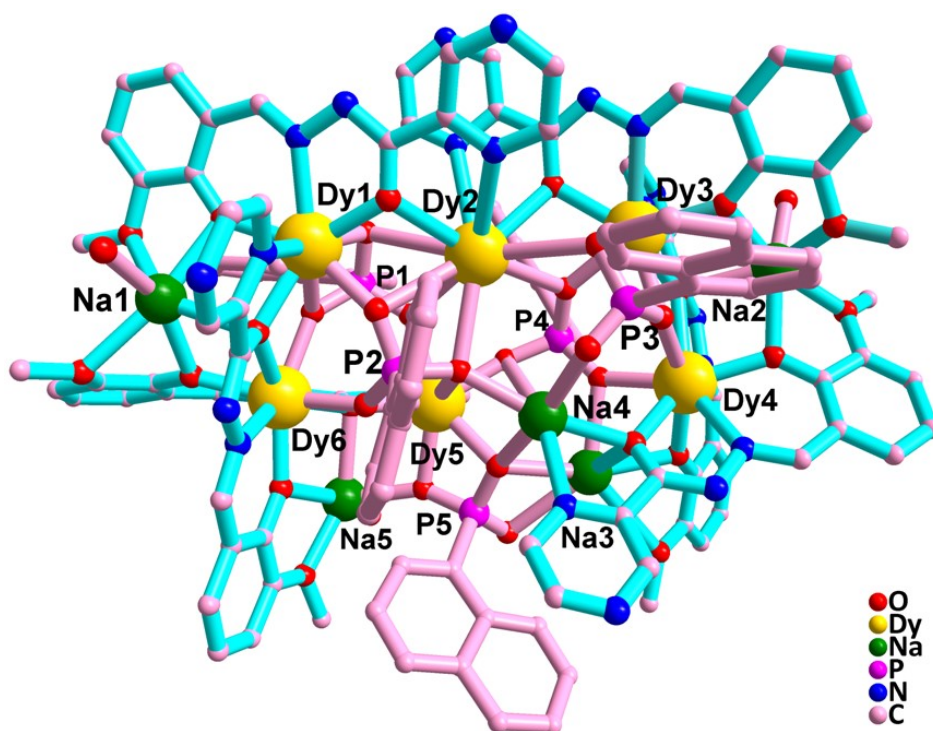


Figure S5. Top-view of **1**. Color scheme: the opch^{2-} fragments in turquoise, the $\text{C}_{10}\text{H}_7\text{PO}_3^{2-}$ fragments in rose, Dy in gold, O in red, N in blue, C in rose, P in pink.

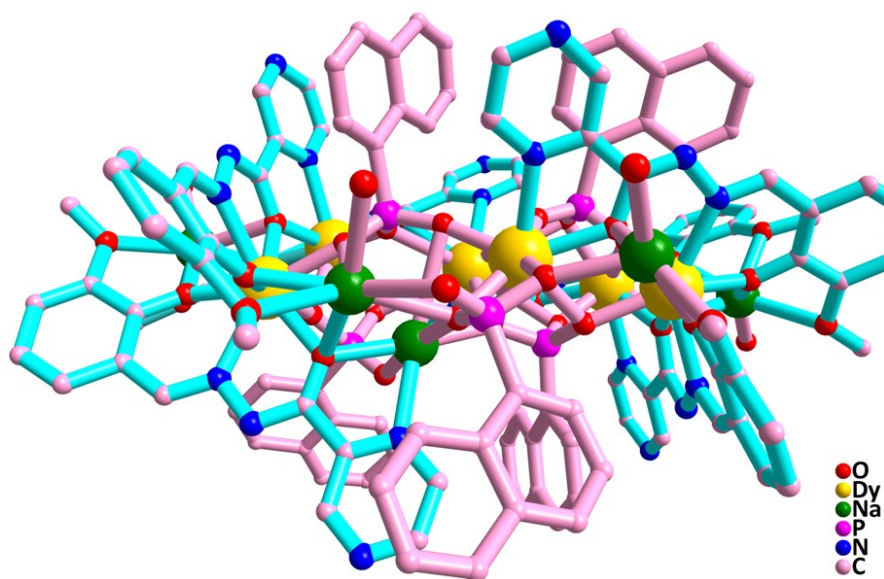


Figure S6. Side-view of **1**. Color scheme: the opch^{2-} fragments in turquoise, the $\text{C}_{10}\text{H}_7\text{PO}_3^{2-}$ fragments in rose, Dy in gold, O in red, N in blue, C in rose, P in pink.

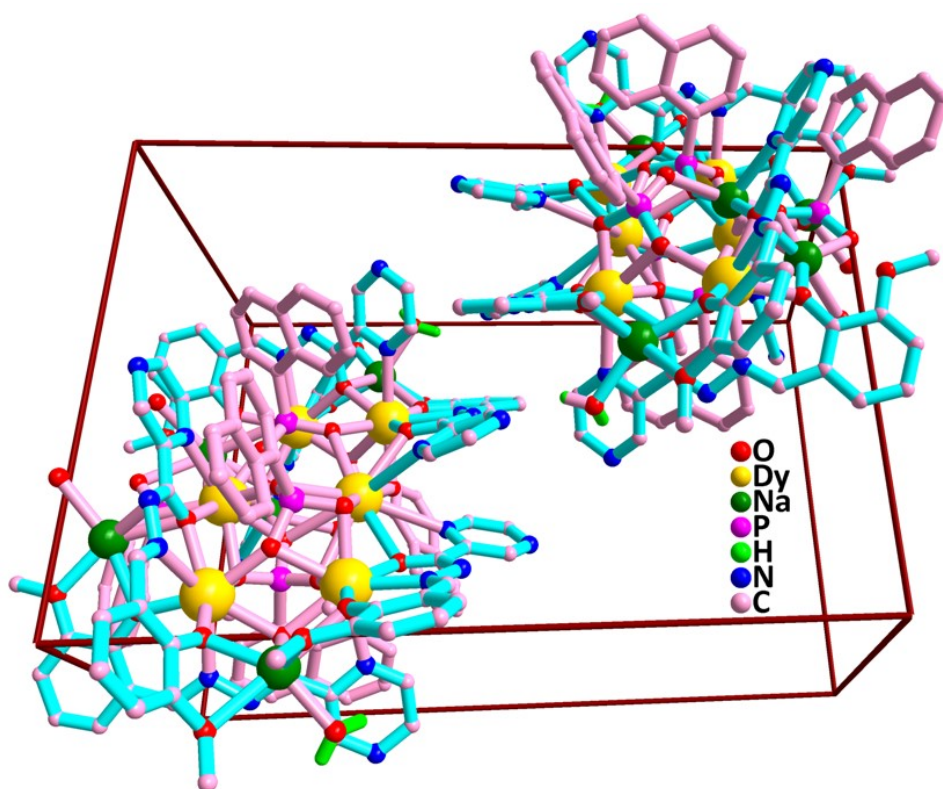


Figure S7. Unit cell of **1** showing the presence of two isomers.

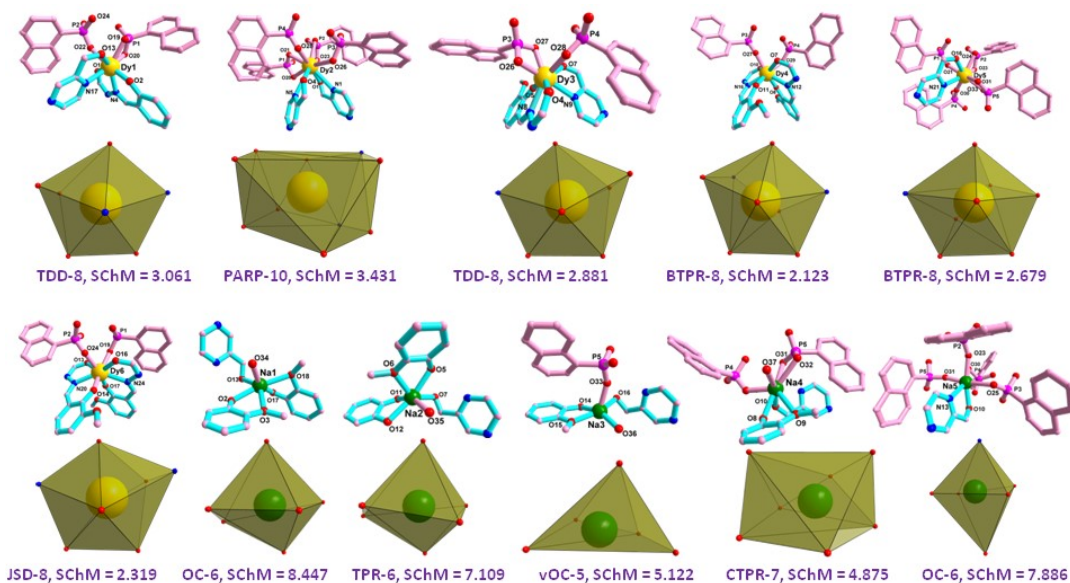


Figure S8. Coordination environments of six crystallographically independent Dy^{III} ions and five Na^I ions in **1**. Color scheme: the opch²⁻ fragments in turquoise, the C₁₀H₇PO₃²⁻ fragments in rose, Dy in gold, O in red, N in blue, C in rose, P in pink.

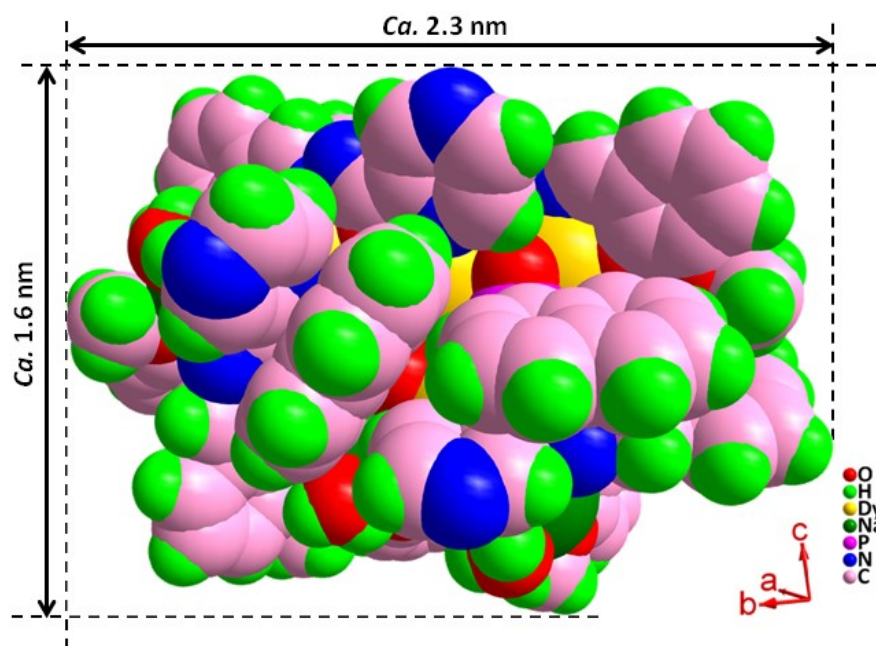


Figure S9. Space-filling representation of **1**. Color scheme: Dy in gold, Na in green, O in red, N in blue, P in pink, C in rose, H in bright green.

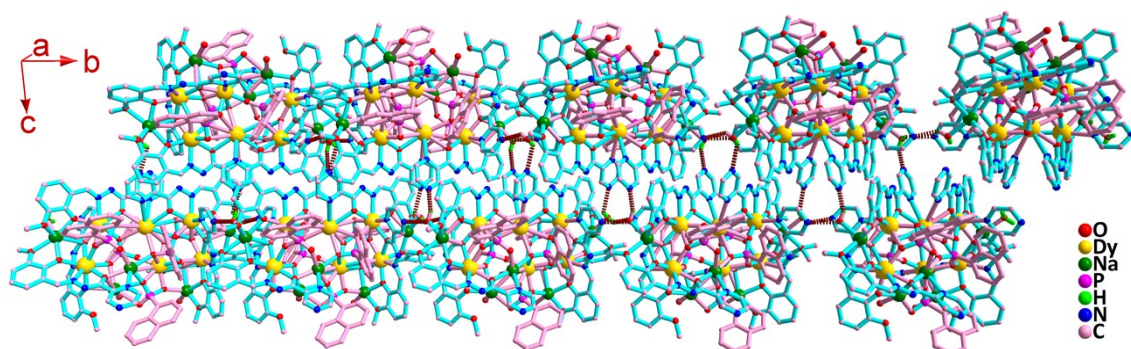
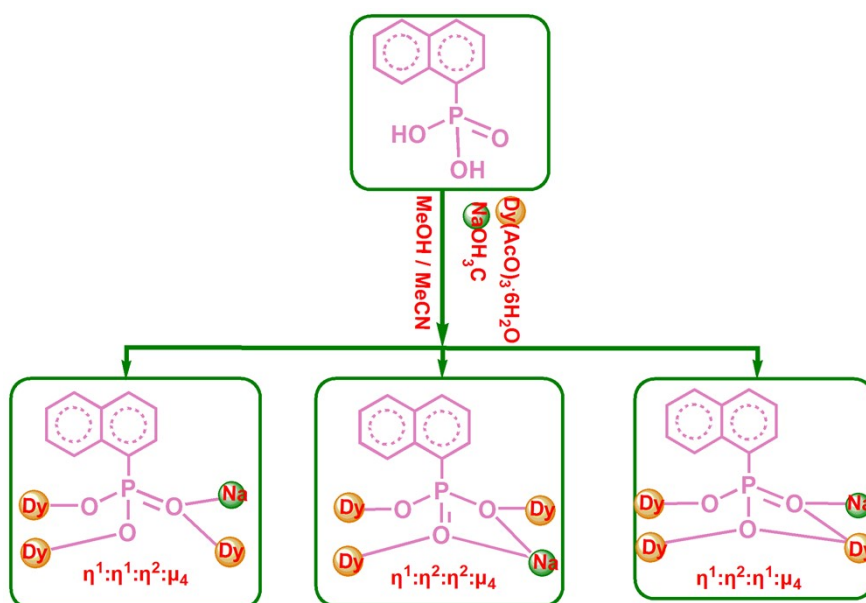
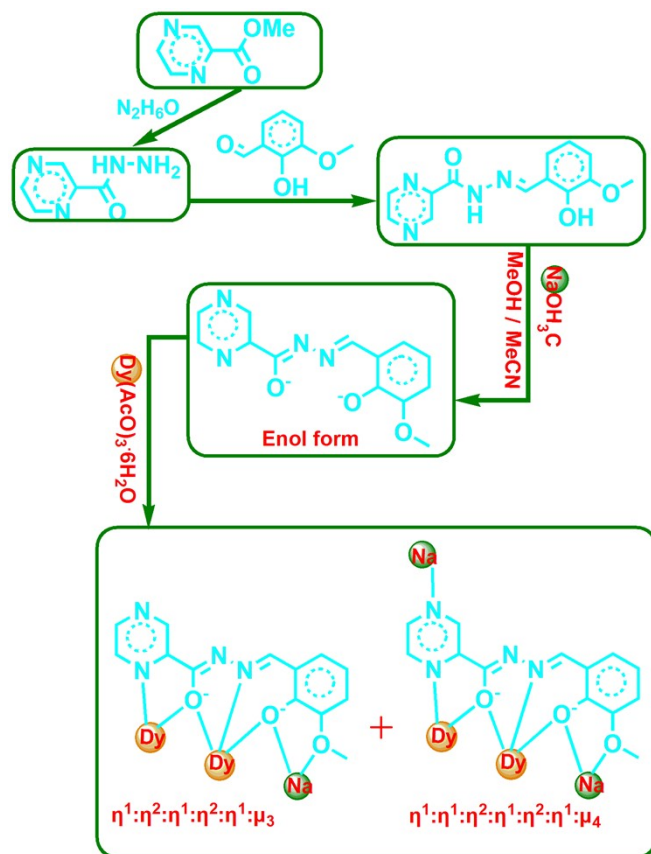


Figure S10. Illustration showing the hydrogen-bonding interactions (brown dash lines) and the double-chain supramolecular arrangement of the molecules in **1**.



Scheme S3. H_2opch , di-deprotonated opch^{2-} and corresponding coordination mode in **2**.



Scheme S4. H_2opch , di-deprotonated opch^{2-} and corresponding coordination mode in **2**.

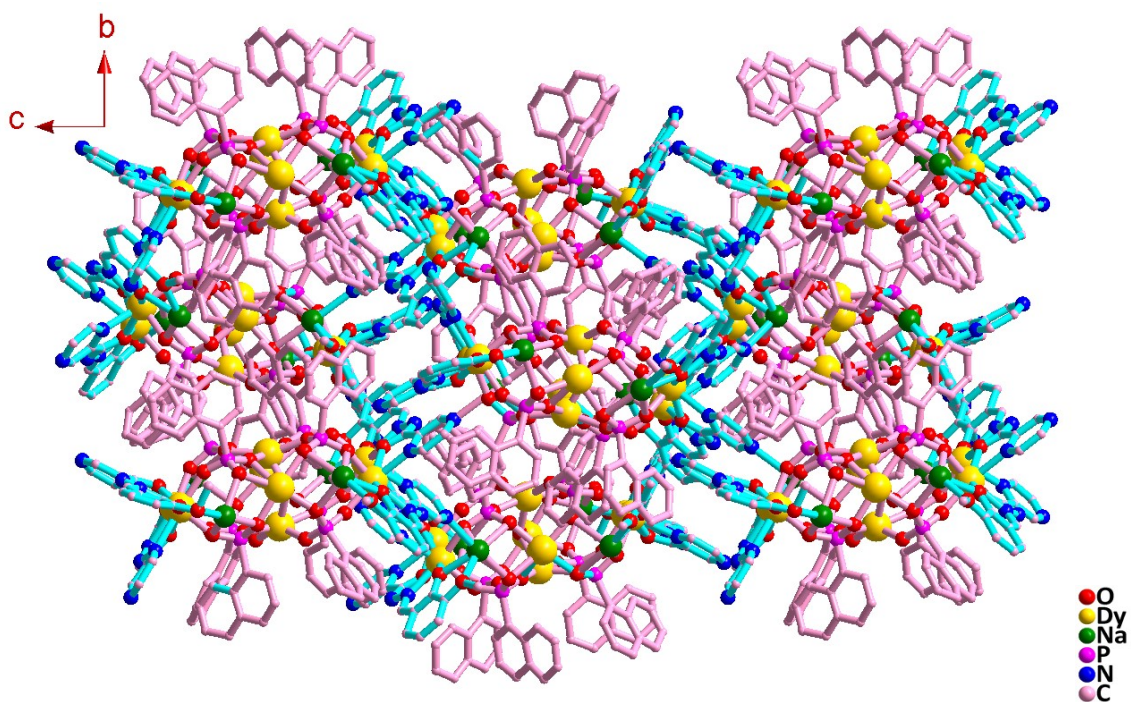


Figure S11. Single-crystal structure of **2**. Color scheme: the opch^{2-} fragments in turquoise, the $\text{C}_{10}\text{H}_7\text{PO}_3^{2-}$ fragments in rose, Dy in gold, O in red, N in blue, C in rose, P in pink.

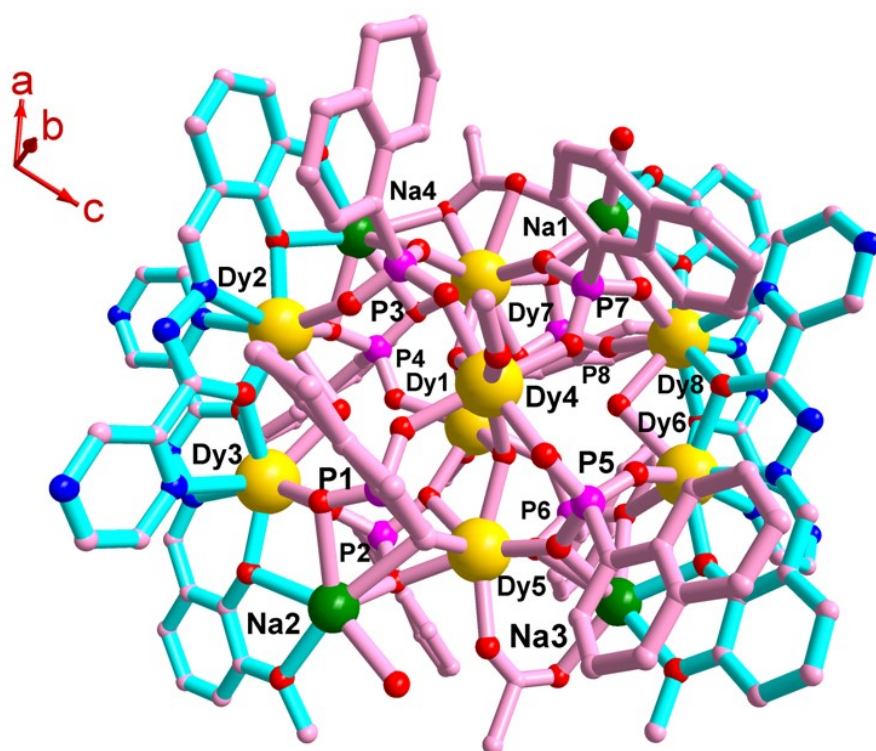


Figure S12. Top-view of **2**. Color scheme: the opch^{2-} fragments in turquoise, the $\text{C}_{10}\text{H}_7\text{PO}_3^{2-}$ fragments in rose, Dy in gold, O in red, N in blue, C in rose, P in pink.

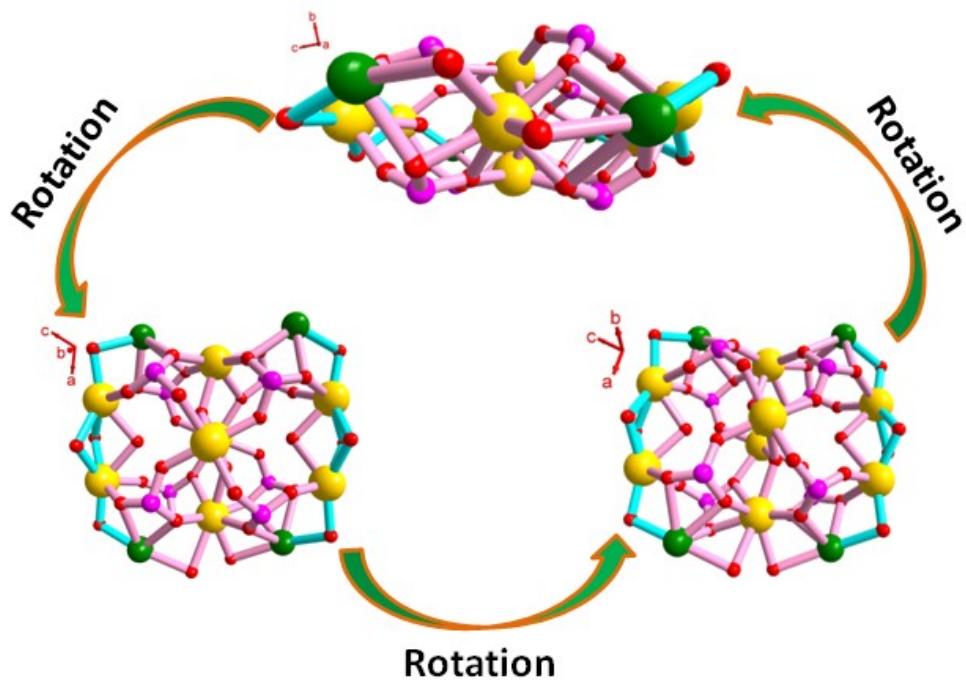


Figure S13. Continuous observation of the Na_4Dy_8 core from top- to side-view in **2**.

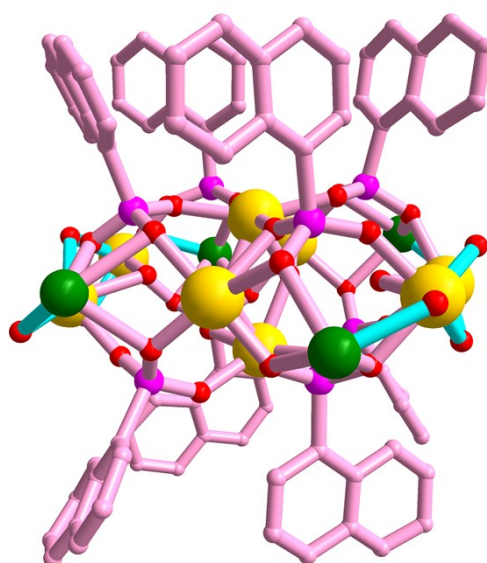


Figure S14. The $[\text{Na}_4\text{Dy}_8(\text{C}_{10}\text{H}_7\text{PO}_3)_8]^{12+}$ core for **2**. Color scheme: the $\text{C}_{10}\text{H}_7\text{PO}_3^{2-}$ fragments in rose, Dy in gold, O in red, C in rose, P in pink.

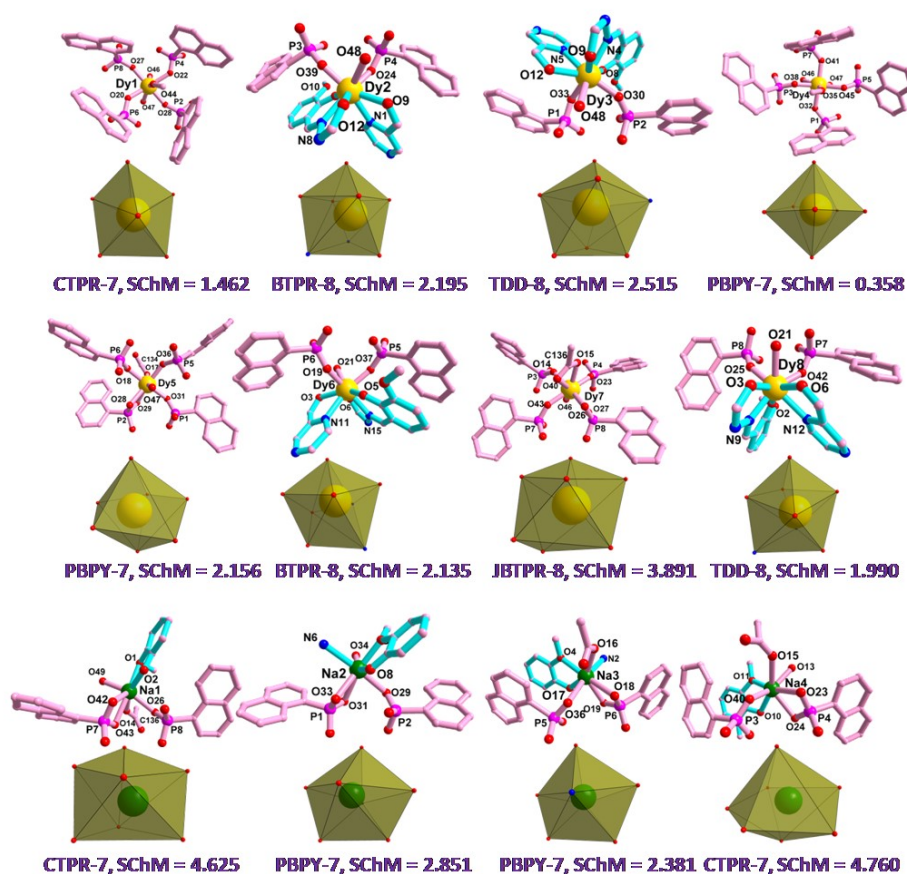


Figure S15. Coordination environments of eight crystallographically independent Dy^{III} ions and four Na^{I} ions in **2**. Color scheme: the opch^{2-} fragments in turquoise, the $\text{C}_{10}\text{H}_7\text{PO}_3^{2-}$ fragments in rose, Dy in gold, O in red, N in blue, C in rose, P in pink.

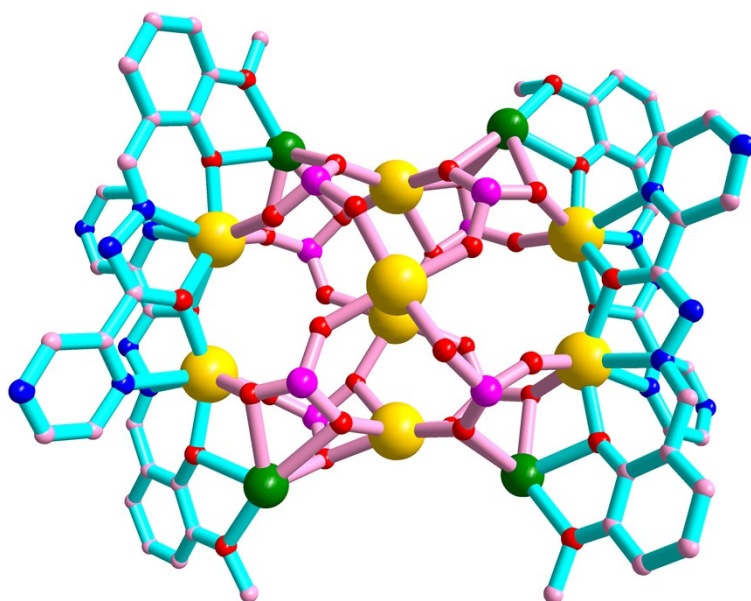


Figure S16. The $[\text{Na}_4\text{Dy}_8(\text{opch})_4(\text{PO}_3)_8]^{4+}$ core for **2**. Color scheme: the opch²⁻ fragments in turquoise, the PO₃²⁻ fragments in rose, Dy in gold, O in red, N in blue, C in rose, P in pink.

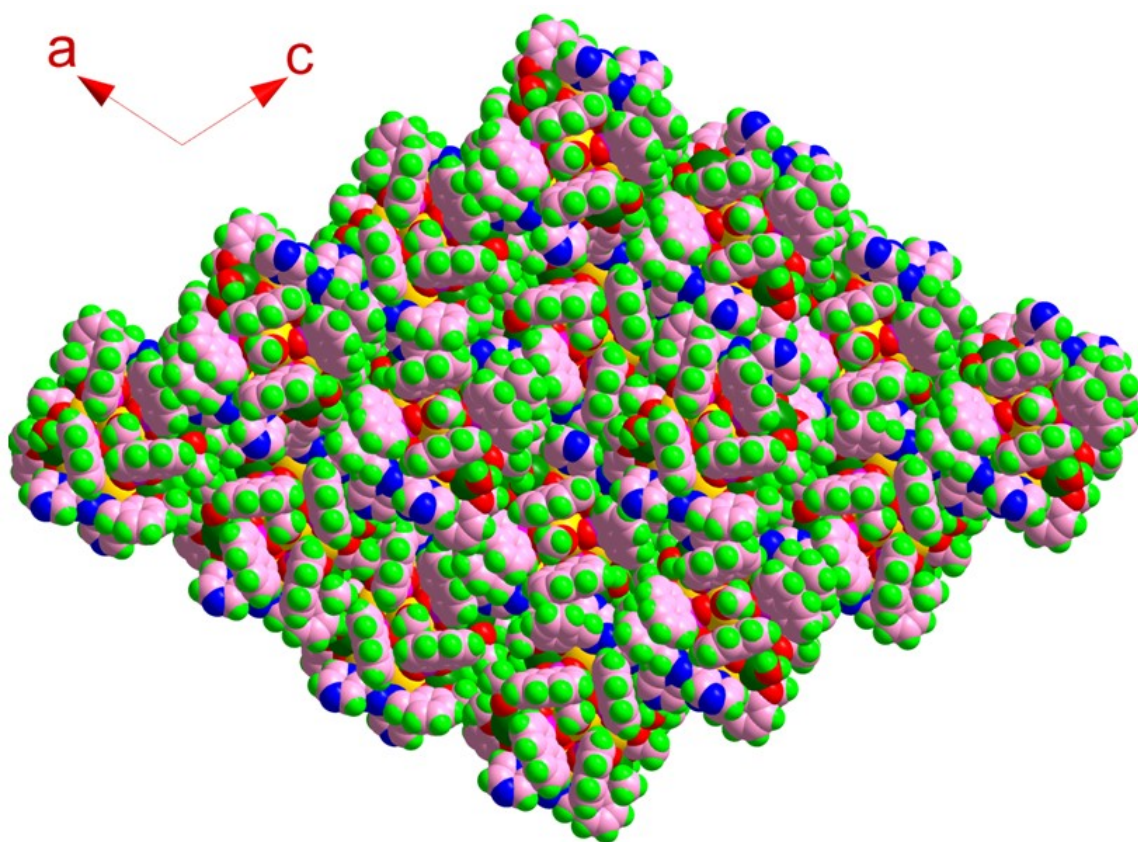


Figure S17. Space-filling representation of **2**. Color scheme: Dy in gold, Na in green, O in red, N in blue, P in pink, C in rose, H in bright green.

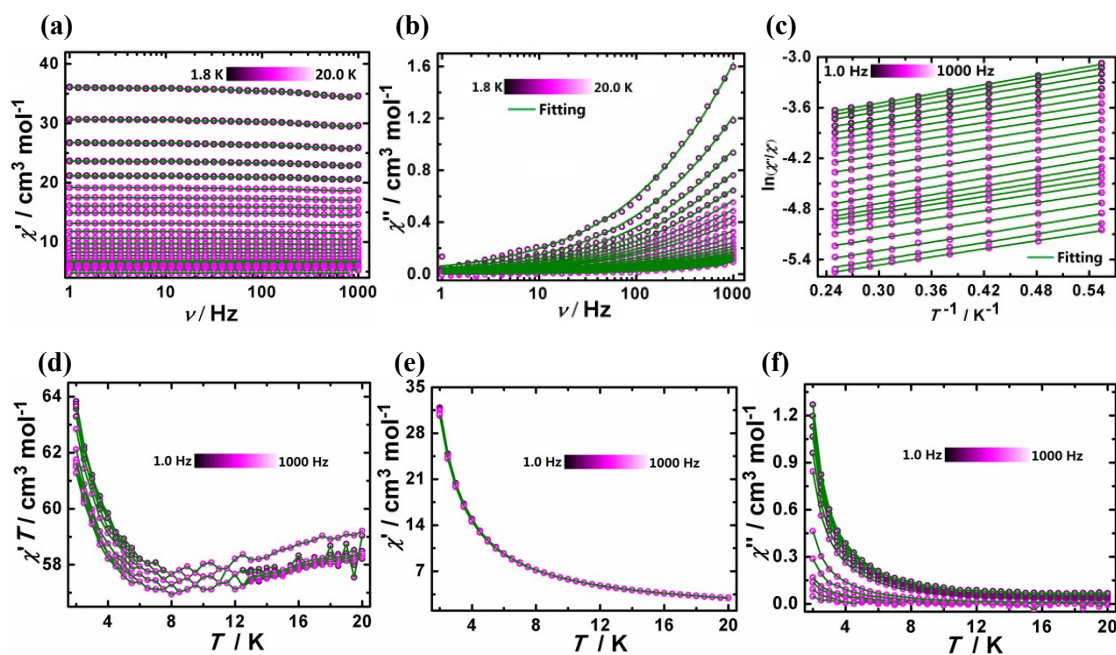


Figure S18. Frequency dependence of the χ' (a) and χ'' (b) products, *ac* susceptibilities under zero *dc* field for **1**. The $\ln(\chi''/\chi')$ versus T^{-1} plots (c). Temperature dependence of the $\chi'T$ (d), χ' (e) and χ'' (f) products, *ac* susceptibilities (MPMS3).

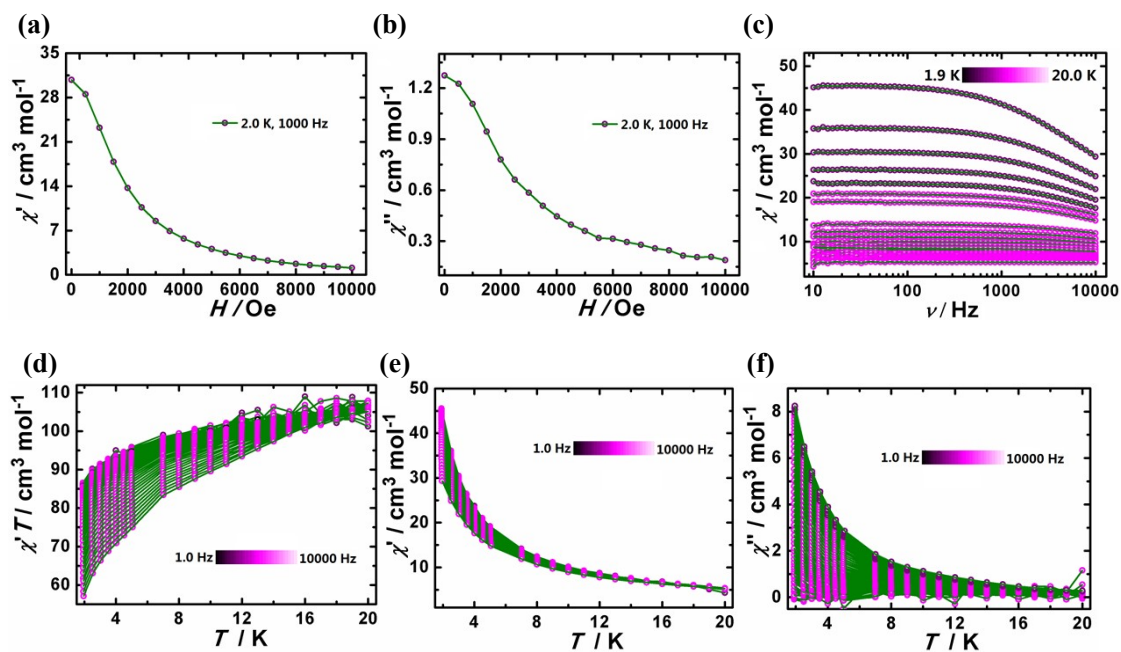


Figure S19. Field dependence of the χ' (a) and χ'' (b) products, *ac* susceptibility of **1** at 1000 Hz and 2 K. Frequency dependence of the χ' (c) product, *ac* susceptibilities under zero *dc* field. Temperature dependence of the $\chi'T$ (d), χ' (e) and χ'' (f) products, *ac* susceptibilities (PPMS).

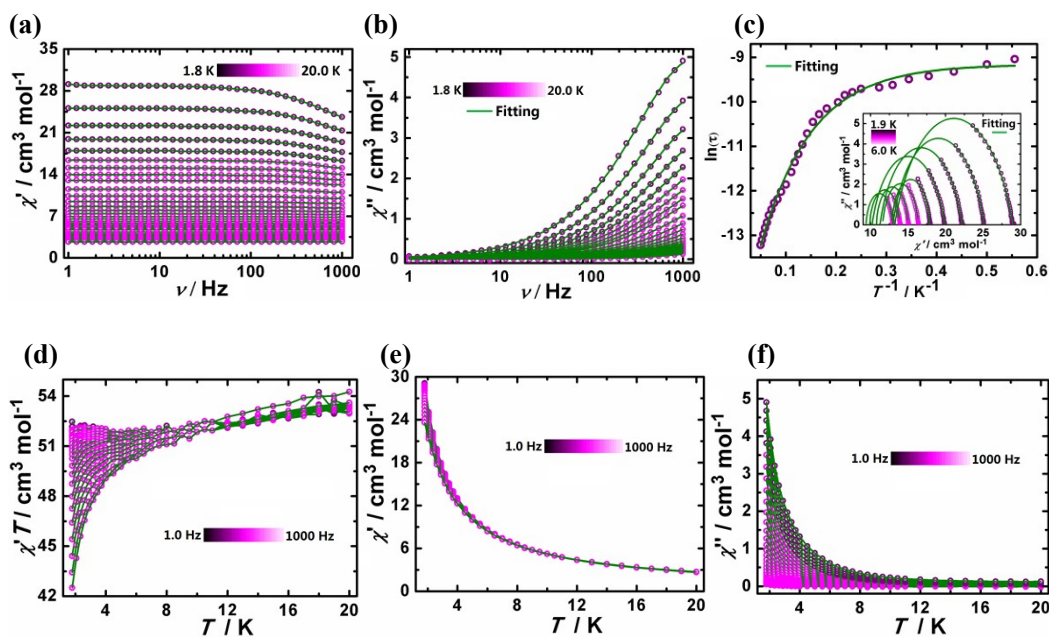


Figure S20. Frequency dependence of the χ' (a) and χ'' (b) products, ac susceptibilities under zero dc field for **2** (MPMS3). The $\ln(\tau)$ versus T^{-1} plots (c). Temperature dependence of the $\chi'T$ (d), χ' (e) and χ'' (f) products, ac susceptibilities (PPMS).

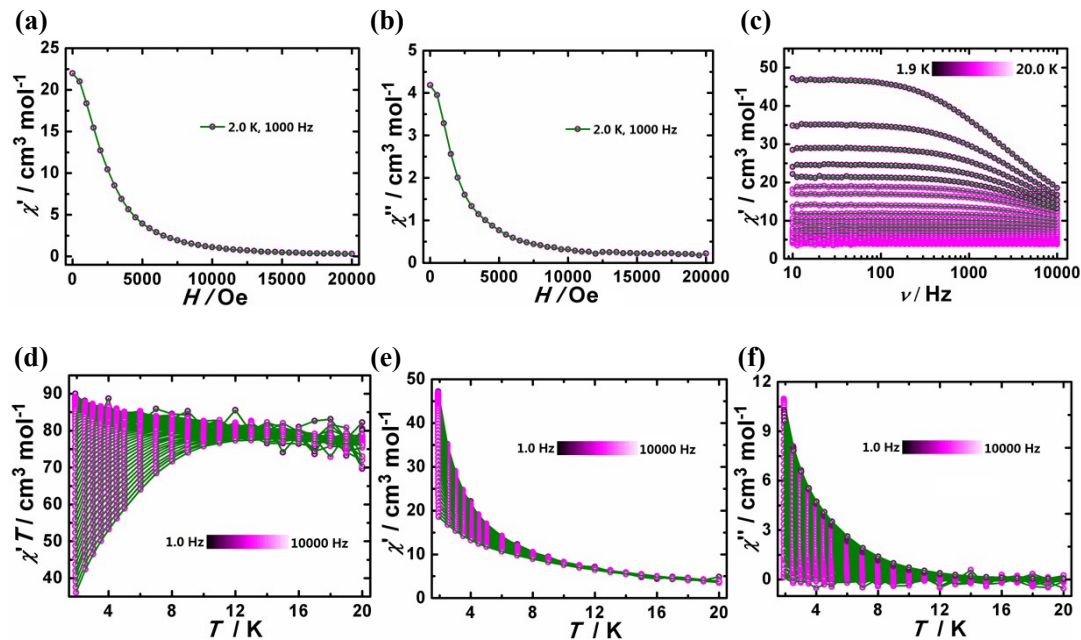


Figure S21. Field dependence of the χ' (a) and χ'' (b) products, ac susceptibility of **2** at 1000 Hz and 2 K. Frequency dependence of the χ' (c) product, ac susceptibilities under zero dc field. Temperature dependence of the $\chi'T$ (d), χ' (e) and χ'' (f) products, ac susceptibilities (PPMS).